CDF note xxxx

# Measurement of the Gluon Fusion Fraction in $t\bar{t}$ Production using Azimuthal Correlation of Charged Leptons


The CDF Collaboration
*URL http://www-cdf.fnal.gov*



(Dated: July 19, 2008)



In the standard model, $t\bar{t}$ pairs are produced mainly through $q\bar{q}$ annihilation and gluon fusion in $p\bar{p}$ collisions at $\sqrt{s} = 1.96$ TeV. We present a measurement of the relative fraction of $t\bar{t}$ production through gluon fusion $f_{gg}$ using an azimuthal correlation of charged leptons in the $t\bar{t}$ dilepton Channel. We use a total integrated luminosity of 2.0 fb$^{-1}$, and find the fraction of gluon fusion $f_{gg} = 0.53\,^{+0.36}_{-0.38}$.

## I. INTRODUCTION

In $p\bar{p}$ collisions at $\sqrt{s} = 1.96$ TeV, $t\bar{t}$ pairs are produced dominantly through $q\bar{q}$ annihilation, while about 15% of $t\bar{t}$ pairs are predicted to be produced via gluon-fusion [1]. Because of uncertainties in the large-$x$ gluon luminosity, the prediction of this fraction has a large ambiguity and will change by up to a factor of 2 (from 10% to 20%). Hence, measurement of the gluon fusion fraction will give the knowledge of the gluon content of the proton at large values of $x$ as well as test for the perturbative QCD calculation of gluon fusion.

$t\bar{t}$ pair produced via gluon fusion has a different spin state from one via $q\bar{q}$ annihilation. This difference manifests itself efficiently as an azimuthal correlation of charged leptons in the $t\bar{t}$ dilepton channel [2]. If we assume $t\bar{t}$ pair production close to threshold, $t\bar{t}$ pair produced via gluon fusion and $q\bar{q}$ annihilation is in the following spin state [3]:

$$\begin{aligned} gg &: J = 0, J_z = 0 \\ q\bar{q} &: J = 1, J_z = \pm 1 \ , \end{aligned}$$

where $z$ denotes the initial parton direction (i.e. nearly the beam direction).

Therefore, in the case of gluon fusion, the top quark and the anti-top quark tend to have the opposite spin on any quantize axis, while the aligned spin on the beam axis in the case of $q\bar{q}$ annihilation.

We utilize the difference in azimuthal correlation of charged leptons in the $t\bar{t}$ dilepton channel to distinguish $t\bar{t}$ pair produced via gluon fusion from $q\bar{q}$ annihilation.

## II. DATA SAMPLE & EVENT SELECTION & BACKGROUND TABLE

This analysis is based on an integrated luminosity of 2.0 fb$^{-1}$ collected with the CDFII detector /citeCDF between March 2002 and March 2007. The data are collected with an inclusive lepton trigger that requires an electron or muon with E$_T$ >18 GeV (P$_T$ >18 GeV/c for the muon). The event signature of $t\bar{t}$ dilepton events is that the event has two high $p_T$ leptons from W decay, large missing $E_T$ due to two missing neutrinos, and two jets originating from $b$-quarks. The selection criteria are described in [4].

- Two electrons or muons with $p_T > 20$ GeV. At least one of them is required to be in the central region and at least one of them must be isolated.
- If the event has a lepton originates from $\gamma$ conversion or a track of cosmic particle, the event is rejected.
- $\not{E}_T > 25$ GeV
- $\not{E}_T > 50$ GeV or the angle between $\not{E}_T$ and any lepton or jet direction projected on the azimuthial plane in the event is required to be greater than 20°
- Two or more jets with level 5 corrected $E_T > 15$ GeV and $|\eta| < 2.5$
- Veto $Z$-events: If the event has same flavor lepton pair with its invariant mass in $76 < M_\ell\ell < 106$ GeV, the missing $E_T$ significance $\not{E}_T/\sqrt{\sum E_T} > 4$
- Scaler sum of $E_T$s of leptons, jets, and missing energy: $H_T > 200$ GeV
- The lepton pair have to have opposite charges.

The dominant background processes remained by DIL selection are diboson production ($WW/WZ/ZZ$), Drell-Yan ($q\bar{q} \to Z^*/\gamma \to ee, \mu\mu, \tau\tau$), and $W$+jets production where one jet is misidentified as a lepton.

The number of $t\bar{t}$ signal and backgrounds expected with the data corresponds to 2.0 fb$^{-1}$ are estimated using Monte Carlo simulation as well as data in control regions, and summarized in Table I.

## III. SIGNAL AND BACKGROUND TEMPLATES

The strategy of the gluon fusion measurement is that we fit composition of expected $\Delta\phi$ distribution of $gg$, $q\bar{q}$, and background with one of data supposing $gg$ fraction as a free fit parameter. Therefore, we introduce the expected $\Delta\phi$ distributions (templates) of $gg$, $q\bar{q}$, and each background process in this section.

| Process | Number of expected events |
|---|---|
| $WW$ | $6.81 \pm 1.17$ |
| $WZ$ | $1.59 \pm 0.26$ |
| $ZZ$ | $1.09 \pm 0.85$ |
| $W\gamma$ | $0.17 \pm 0.18$ |
| Drell-Yan($Z \to ee, \mu\mu$) | $12.78 \pm 2.17$ |
| $Z \to \tau\tau$ | $5.26 \pm 1.02$ |
| Fakes | $21.75 \pm 6.33$ |
| Total background | $49.45 \pm 7.83$ |
| $t\bar{t}(\sigma = 6.7$ pb) | $93.86 \pm 7.14$ |
| Total SM expectation | $143.31 \pm 13.09$ |
| Data (2.0 fb$^{-1}$) | 145 |

TABLE I: The table of expected number of events in data correspond to 2.0 fb$^{-1}$ with the observed number of events.

### A. Gluon fusion and $q\bar{q}$ annihilation

To obtain $\Delta phi$ in the gluon fusion and $q\bar{q}$ annihilation, we use $t\bar{t}$ pair production Monte Carlo simulation sample which is generated by HERWIG [9] event generator and CDF detector simulator with top quark mass $M_t = 175\ GeV$. In this simulation sample, CTEQ5L set is used as the parton distribution function of proton and anti-proton, and we find about 5% of the sample comes from gluon fusion and the rest comes from $q\bar{q}$ annihilation according to initial state partons.

We separate $t\bar{t}$ events via gluon fusion from $q\bar{q}$ annihilation, and obtain $\Delta\phi$ distributions of $gg$ and $q\bar{q}$ events after DIL selection, separately. Figure 1 shows the distributions of $gg$ (right) and $q\bar{q}$ (left). The histograms are fitted with the following function:

$$\mathcal{F}_i = (3 - P_i^0 cos(\Delta\phi) + P_i^1 cos(2\Delta\phi) + P_i^2 cos(3\Delta\phi))/3\pi, \tag{1}$$

where $P_i^{(n)}$s indicate fitting parameters and the suffix $i$ represent the process, i.e. $i = gg, q\bar{q}$ here. We adopt the function composed with cosine since $\Delta\phi$ distribution should be periodic. The solid curve in the figure indicate the best fit results.

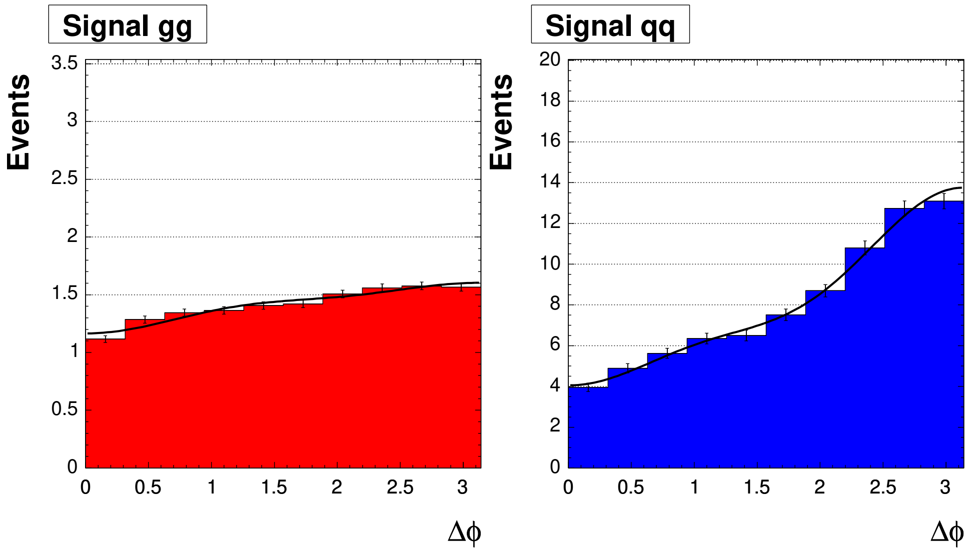


FIG. 1: The distributions of $\Delta\phi$ of gluon fusion (left) and $q\bar{q}$ annihilation (right). The total number in each histogram is normalized to expectation assuming 6.7 pb $t\bar{t}$ cross section. The error bars originate from Monte Carlo statistics. The solid curves in the figure indicate the fit results with the function in the text.

### B. Background

We make $\Delta\phi$ distribution of each background process separately.

For diboson ($WW$, $WZ$, and $ZZ$) events and $Z \to \tau\tau$ events, we rely on MC simulation samples which are generated with PYTHIA [8] event generator.

For Drell-Yan ($Z \to ee, \mu\mu$) events, we also rely on MC simulation samples, but which are generated with Alpgen event generator.

For $W\gamma$ events, we ignore the background from this process, since the contribution from $W\gamma$ to background are negligibly small.

For fake events, i.e. one lepton with jets events where one of jets is misidentified as another lepton, we use a real event which contains a lepton and at least one "fakeable" jet and make one of the jets in an events forcibly to be mis-reconstructed as an electron or a muon. In this case, the event weight is not unit, but is adopted to be their fake rate.

$\Delta\phi$ histograms of background above are summed up with weights according to their expected number of events in Table I. Then we fit the distribution to Eqn. (1).

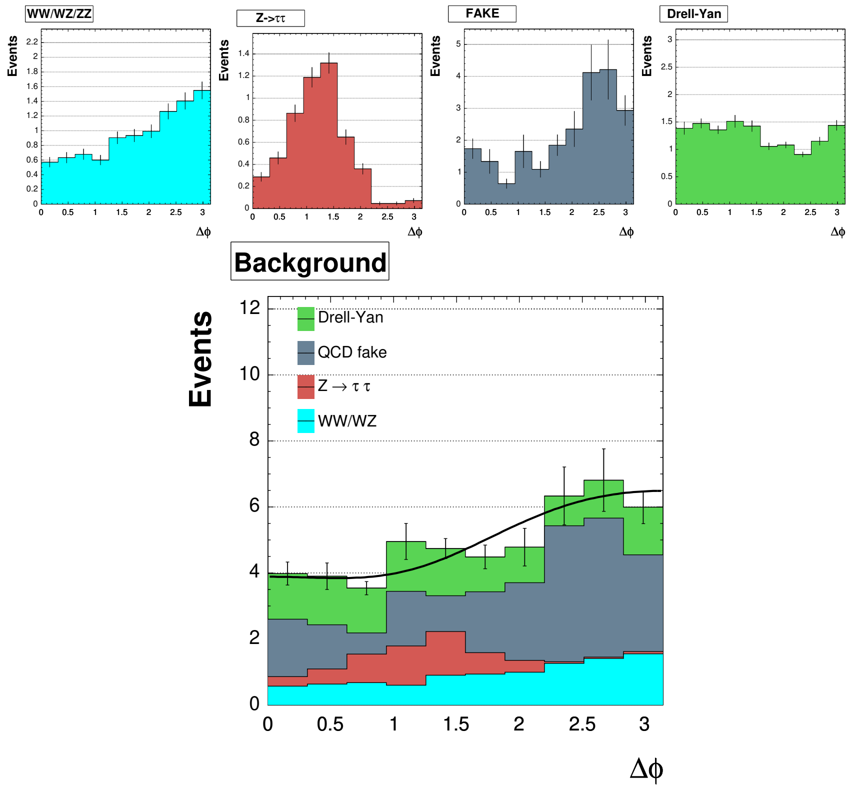


FIG. 2: The distributions of $\Delta\phi$ of diboson ($WW$, $WZ$, and $ZZ$) processes, $Z \to \tau\tau$, Drell-Yan ($Z \to ee, \mu\mu$), fake events, and all background events from above four components. The total number in each histogram is normalized to each expected number at 2.0 fb$^{-1}$ data. The error bars originate from statistics. The solid curve in the figure (e) indicates the fit results to the function in the text.

We summarize the fit result of parameters in Table II. $\chi^2$/ndf of the fits are in the table as well.

| Source | $P^0$ | $P^1$ | $P^2$ | $\chi^2$/ndf |
|---|---|---|---|---|
| $gg$ | $0.39 \pm 0.03$ | $0.06 \pm 0.06$ | $0.07 \pm 0.07$ | 13.7/7 |
| $q\bar{q}$ | $1.57 \pm 0.05$ | $-0.33 \pm 0.05$ | $0.25 \pm 0.05$ | 6.7/7 |
| background | $0.85 \pm 0.11$ | $-0.14 \pm 0.11$ | $-0.07 \pm 0.11$ | 11.6/7 |

TABLE II: The fit result of parameters, together with $\chi^2$/ndf.

## IV. DETERMINATION OF $gg$ FRACTION

We define an unbinned likelihood as follows:

$$\mathcal{L}(\mathcal{F}_{gg}, n_\mathrm{s}) \equiv \prod_i \frac{n_\mathrm{s} f_{t\bar{t}}(\Delta\phi_i; \mathcal{F}_{gg}) + n_\mathrm{b} f_\mathrm{b}(\Delta\phi_i)}{n_\mathrm{s} + n_\mathrm{b}}$$

$$f_{t\bar{t}}(\Delta\phi_i; \mathcal{F}_{gg}) \equiv \frac{\mathcal{F}_{gg} f_{gg}(\Delta\phi_i) + (1 - \mathcal{F}_{gg}) f_{q\bar{q}}(\Delta\phi_i)}{\mathcal{F}_{gg} + (1 - \mathcal{F}_{gg})} ,$$

where $\mathcal{F}_{gg}$ and $n_\mathrm{s}$ are assumed $gg$ fraction and number of $t\bar{t}$ events, respectively. $\Delta\phi_i$ denotes $\Delta\phi$ observed in the $i$-th candidate event. $N$ is the total number of candidate events, and $n_\mathrm{b}$ indicates the expected number of background events. The functions $f_{gg}$, $f_{q\bar{q}}$, and $f_\mathrm{b}$ are probability density of $\Delta\phi$ for $gg$, $q\bar{q}$, and background events, which are obtained in Sec.III, respectively. We take $\mathcal{F}_{gg}$ which maximizes this likelihood as the observed $gg$ fraction, and describe this as $\mathcal{F}_{gg}^{\mathrm{measured}}$ hereafter.

### A. Sensitivity by pseudo-experiments

Next, we perform pseudo-experiments to look how an observed $\mathcal{F}_{gg}$ distributes for the assumption of true $\mathcal{F}_{gg}$.

In each pseudo-experiment, we generate $N$ random numbers distribute the probability density function $n_\mathrm{s}\left\{\mathcal{F}_{gg} f_{gg} + (1 - \mathcal{F}_{gg}) f_{q\bar{q}}\right\} + n_\mathrm{b} f_\mathrm{b}$, where we assume $n_\mathrm{b}$ is the center value of estimated number of background events, and $n_\mathrm{s}$ is $N - n_\mathrm{b}$. The uncertainty in $n_\mathrm{b}$ is considered later as a systematic error.

We perform 10,000 pesudo-experiments for each assumption of $\mathcal{F}_{gg}$, and obtain the observed $\Delta phi$ as the best fit of the likelihood function Eqn. (2) from each pesudo-experiment. We extract the mean value and sigma of the distribution from Gaussian fitting for each assumed $\mathcal{F}_{gg}$. Figure 3 shows the mean value of the observed $\Delta\phi$ distribution (left) and residual (center), and its gisma(right), as a function of the input $\mathcal{F}_{gg}$ of the pseudo-experiments. The figure indicates

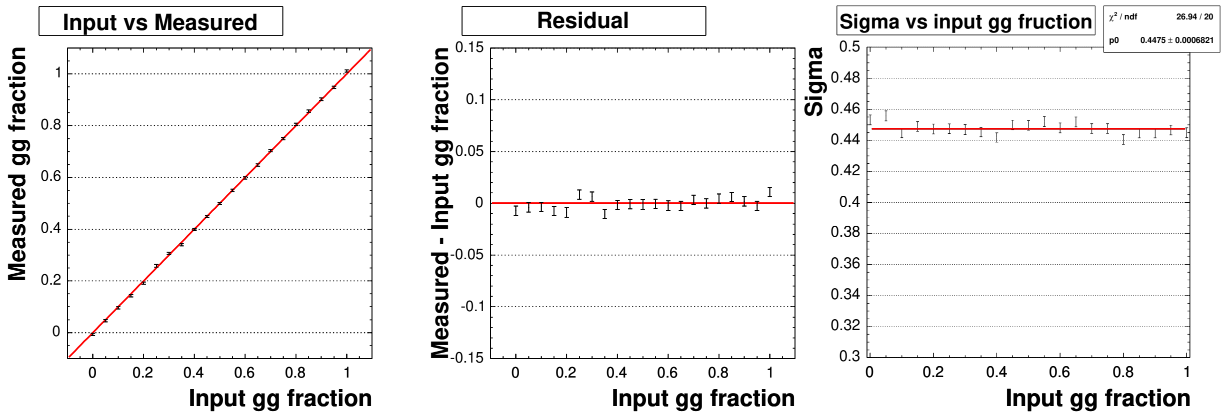


FIG. 3: The mean value of the observed $\Delta\phi$ distribution (left) and its sigma (right) as a function of the input $\mathcal{F}_{gg}$ of the pseudo-experiments with $N = 145$.

that the measurement has a good linearity of response for the input $\mathcal{F}_{gg}$ and sensitivity of the measurement is about 44.8% almost independent of input $\mathcal{F}_{gg}$.

## V. SYSTEMATIC UNCERTAINTIES

We discuss here about possible systematic uncertainties and integrate them into F-C confidence belt. We consider the following systematics source:

- Shapes of $\Delta\phi$ templates and Expected number of background.
- Acceptance ratio of $gg$ to $q\bar{q}$.
- Estimation method of systematic uncertainty.

- Theoretical calculation of $t\bar{t}$ pair production matrix element.
- Initial/Final state radiation.
- Parton distribution function.
- Other systematics

### A. $\Delta\phi$ templates and Expected number of background

The $\Delta\phi$ distributions of $gg$, $q\bar{q}$, and background are obtained by fitting the histograms to the function Eqn. (1) in Sec. III.

And the expected number of background is used in the likelihood function defined in Eqn. (2). Consequently uncertainty in expected number of background is one of systematics sources.

In order to look the effect by uncertainties of the $\Delta\phi$ template of $gg$, $q\bar{q}$ and background, we generate 10,000 sets of pseudo-data with each for $\mathcal{F}_{gg}^{\rm true}$, where each bin's uncertainty of statistics for the shape systematics due to MC statistics, and each background number. Generally we use function that fitted results of each $\Delta\phi$ template to make pseudo data, but in this systematic estimation we use gg fusion, qq annihilation and each background histogram.

Then, we perform the measurement of $\mathcal{F}_{gg}^{\rm measured}$ on the assumption of center values for expected number of background, and look how much shift in sigma of $\mathcal{F}_{gg}^{\rm measured}$ is observed. We take a quadratic increment of sigma as a systematic uncertainty. We didn't see any obvious dependence on $\mathcal{F}_{gg}^{\rm true}$, so quote 5.0% due to $\Delta\phi$ templates and Expected number of background.

### B. Acceptance ratio of $gg$ to $q\bar{q}$

Acceptance ratio of $gg$ to $q\bar{q}$, $\mathcal{R} = A_{gg}/A_{q\bar{q}}$, is a direct function to the $\mathcal{F}_{gg}^{\rm measured}$. Consequently uncertainty in $\mathcal{R}$ is one of systematics sources. We used $t\bar{t}$ Monte Carlo data (htop75 and self generated gg fusion 100% sample) which is generated by HERWIG event generator and CDF detector simulation to obtain the acceptance ratio, $\mathcal{R}$, and found $\mathcal{R} = 1.013 \pm 0.014$. We didn't see any obvious difference between gg and qq, so just quote the 14% systematic uncertainty due to uncertainties in $\mathcal{R}$.

### C. Estimation Method of Systematic Uncertainty

We use generator level information, i.e. not full simulatied data, for the $\Delta\phi$ distribution of systematic sample to get high statistics. And also, we use below the equation for the $\Delta\phi$ distribution of systematic sample.

$$f_i^{\rm Systematic}(\Delta\phi) \equiv \frac{f_i^{\rm Systematic,hepg}(\Delta\phi)}{f_i^{\rm Default,hepg}(\Delta\phi)} f_i^{\rm Default,FullSim}(\Delta\phi)$$

Basically difference between hepg and full simulation get cancel out. But if this difference is change between gg fusion and qq annihilation by systematic source, we should consider about that difference. But we don't have enough statistics on systematics sample to look this difference. Therefore we add difference between hepg and full simulation as a systematic uncertainty due to estimation method of systematic uncertainty. We generate 10,000 sets of pseudo-data in each $\mathcal{F}_{gg}^{\rm true}$, where $\Delta\phi$ templates of $qq$ and $q\bar{q}$ are changed to the templates obtained by the weighted MC method on the difference between hepg and full simulation, and look how much shift in $\mathcal{F}_{gg}^{\rm measured}$ is observed. Figure 4 shows resulting shifts. Systematics uncertainty due to the difference between hepg and full simulation is Table III.

### D. Theoretical calculation of $t\bar{t}$ pair production matrix element

In this analysis, we rely on the matrix elements of $gg \to t\bar{t}$ and $q\bar{q} \to t\bar{t}$ in HERWIG event generator where LO $t\bar{t}$ matrix element with the spin correlations are taken into account. One could find the effect of NLO calculation of the matrix elements in Ref [5].

We examine the effect of NLO matrix elements for $\Delta\phi$ templates of $gg$ and $q\bar{q}$ using MC@NLO version 3.3 event generator [6]. MC@NLO takes the spin correlation in $t\bar{t}$ into account correctly since this version.

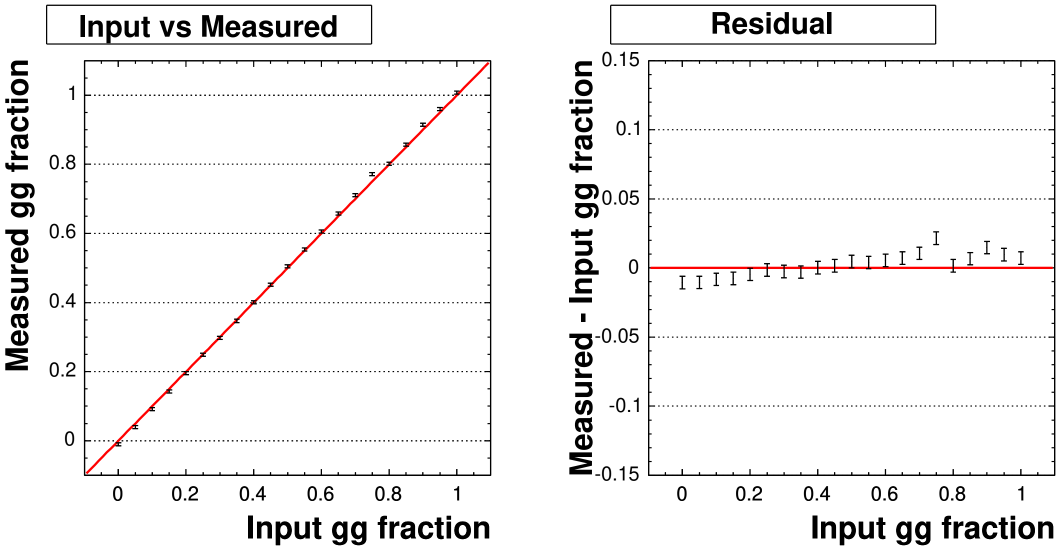


FIG. 4: Linearity and residual plot of input $gg$ vs measured $gg$ fraction for systematic uncertainty of Top $P_T$ difference between HERWIG and PYTHIA. The solid line indicate the fit by linear function.

Because leptons are well reconstructed, especially in their direction, $\Delta\phi$ is hardly affected by smearing in the reconstruction. Therefore, we postulate that the ratio of $\Delta\phi$ distributions of our toy MC events is applicable to distributions of the full detector simulated events, i.e. to obtain $\Delta\phi$ templates, we don't need full detector simulation, but generator level events are enough.

Here we obtain the ratio of $\Delta\phi$ probability density function by MC@NLO ($f_i^{\rm NLO,hepg}(\Delta\phi)$, $i = gg, q\bar{q}$) to by HERWIG ($f_i^{\rm LO,hepg}(\Delta\phi)$), and apply the ratio to the default templates $f_i(\Delta\phi)$ to infer templates by MC@NLO ($f_i^{\rm NLO}(\Delta\phi)$), i.e.

$$f_i^{\rm NLO}(\Delta\phi) \equiv \frac{f_i^{\rm NLO,hepg}(\Delta\phi)}{f_i^{\rm LO,hepg}(\Delta\phi)} f_i(\Delta\phi)$$

We generate 10,000 sets of pseudo-data in each $\mathcal{F}_{gg}^{\rm true}$, where $\Delta\phi$ templates of $qq$ and $q\bar{q}$ are changed to $f_i^{\rm NLO}(\Delta\phi)$, respectively. Then, we perform the measurement of $\mathcal{F}_{gg}^{\rm measured}$ on the assumption of the default $\Delta\phi$ templates, and look how much shift in $\mathcal{F}_{gg}^{\rm measured}$ is observed. Figure 5 shows resulting shifts. We see obvious dependence on $\mathcal{F}_{gg}^{\rm true}$, so we quote the asymmetric systematics uncertainty of linear function. Systematics function due to NLO effect of the $t\bar{t}$ production matrix elements is Table III.

### E. ISR/FSR

Differences due to QCD initial and final state radiations (ISR and FSR) are estimated using specially generated PYTHIA samples in which the QCD parameters for the parton shower evolution are varied based on the studies of the CDF Drell-Yan data and recommendations from the authors of PYTHIA. Only difference of acceptance ratio of $gg$ to $q\bar{q}$ is considered in Sec. V B.

For ISR/FSR uncertainty, if a gluon is emitted in initial state of $t\bar{t}$ state, the $t\bar{t}$ system will have extra $p_T$, and $\Delta\phi$ is distorted. Therefore, ISR uncertainty may affect $gg/q\bar{q}$ templates. We used hepg information of itoprk and itoprl of more and less ISR/FSR sample. A $t\bar{t}$ event generated by PYTHIA doesn't have the correct spin correlation, but we are interested only in the distortion on a $\Delta\phi$ distribution caused by ISR/FSR uncertainty. Therefore we obtain the ratio of $\Delta\phi$ from more or less ISR/FSR sample to one from the sample with default parameters, and apply the ratio to the default $gg/q\bar{q}$ templates to infer templates with more or less ISR/FSR. Here we obtain the ratio of $\Delta\phi$ probability density function with more or less ISR/FSR settings to default settings and apply the ratio to the default templates to get new templates for more or less ISR/FSR settings ($f_i^{\rm more}(\Delta\phi)$ and $f_i^{\rm less}(\Delta\phi)$). Then, we generate 10,000 sets of pseudo-data in each $\mathcal{F}_{gg}^{\rm true}$, where $\Delta\phi$ templates of $qq$ and $q\bar{q}$ are changed to $f_i^{\rm more}(\Delta\phi)$ and $f_i^{\rm less}(\Delta\phi)$, respectively. Next, we perform the measurement of $\mathcal{F}_{gg}^{\rm measured}$ on the assumption of the default $\Delta\phi$ templates, and look how much shift in $\mathcal{F}_{gg}^{\rm measured}$ is observed.

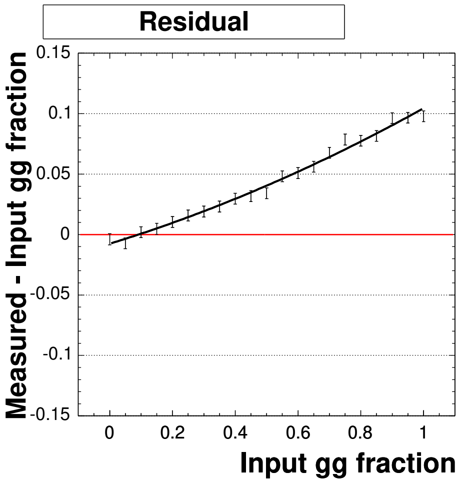


FIG. 5: Residual plot of input $gg$ vs measured $gg$ fraction for systematic uncertainty of Theoretical calculation of $t\bar{t}$ pair production matrix el2ement. The solid line indicate the fit by linear function.

Figure 6 shows resulting shifts. In most of gg fraction both ISR/FSR less and more systematic uncertainty is negative, we quote the half of the largest difference from default value in each input gg fraction. Systematics function due to ISR/FSR more and less is Table III.

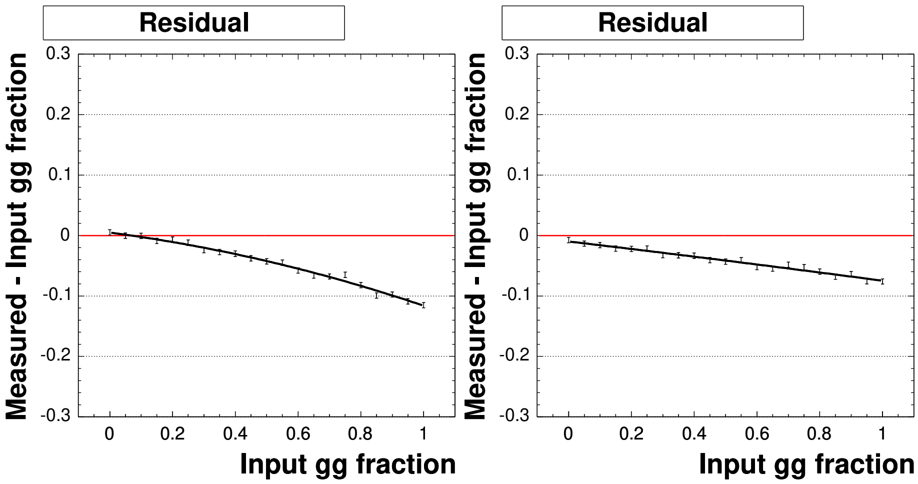


FIG. 6: Residual plot of input $gg$ vs measured $gg$ fraction for systematic uncertainty of ISR/FSR more(left), and ISR/FSR less(right). The solid line indicate the fit by linear function.

### F. Parton Distribution Function

The CTEQ5L parton distribution function (PDF) is used in this analysis. To evaluate the systematics due to PDF uncertainties, we calculate variation in $\Delta\phi$ templates of $gg$ and $q\bar{q}$ when we choose different PDF sets, such as MRST72, MRST75, CTEQ6L, CTEQ6L1 and CTEQ6M. To calculate $\Delta\phi$ templates with different PDF sets, we adopt the weighted MC methodIn this method, we reweigh each event of a MC sample we already have, instead of generating a different set of MC events with each different PDF set. We calculate the relative probability of the event on the assumption of a different PDF set, based on the parton momentum fractions $x_1$, $x_2$, and $Q^2$ in the event, and obtain new templates by re-weighting $\Delta\phi$ distributions.

We generate 10,000 sets of pseudo-data in each $\mathcal{F}_{gg}^{\rm true}$, where $\Delta\phi$ templates of $qq$ and $q\bar{q}$ are changed to the templates obtained by the weighted MC method on the assumption of various PDF sets, respectively. Then, we perform the measurement of $\mathcal{F}_{gg}^{\rm measured}$ on the assumption of the default $\Delta\phi$ templates, and look how much shift in $\mathcal{F}_{gg}^{\rm measured}$ is observed. Figure 7 shows resulting shift by PDF uncertainty. The sum in quadrature of the systematics from the uncertainties of MRST, $\alpha_s$, and 20 parameters is Table III.

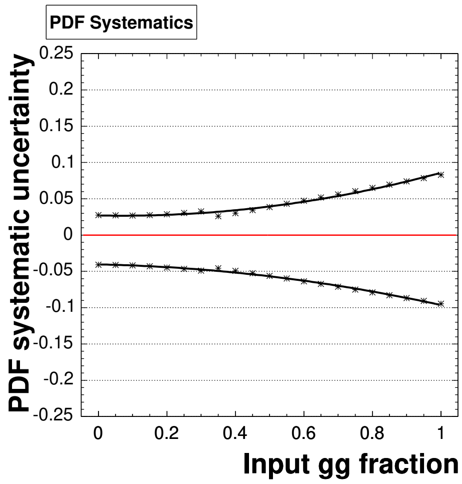


FIG. 7: Residual plot of input $gg$ vs measured $gg$ fraction for systematic uncertainty of PDF. The solid line indicate the fit by linear function.

## G. Other Systematics

We add the systematic uncertainty due to the Top $P_T$ difference between PYTHIA and HERWIG. Top quark $P_T$ difference make difference of leptons $\Delta\phi$. We generate 10,000 sets of pseudo-data in each $\mathcal{F}_{gg}^{\rm true}$, where $\Delta\phi$ templates of $qq$ and $q\bar{q}$ are changed to the templates obtained by the weighted MC method on the difference between PYTHIA and HERWIG, and look how much shift in $\mathcal{F}_{gg}^{\rm measured}$ is observed.

Figure 8 shows resulting shifts. Systematics uncertainty due to the Top $P_T$ difference between HERWIG and PYTHIA is Table III.

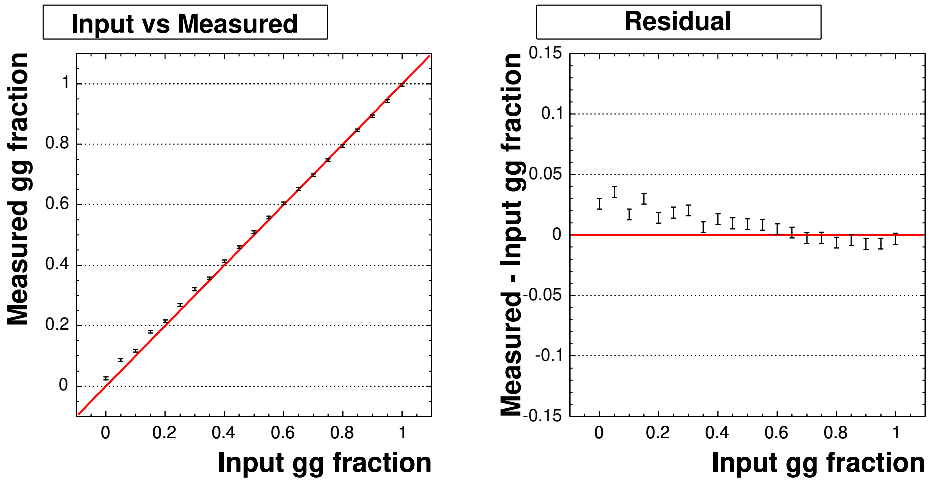


FIG. 8: Linearity and residual plot of input $gg$ vs measured $gg$ fraction for systematic uncertainty of Top $P_T$ difference between HERWIG and PYTHIA. The solid line indicate the fit by linear function.

| Source | Positive Uncertainty in $\mathcal{F}_{gg}^{\text{measured}}$ | Negative Uncertainty in $\mathcal{F}_{gg}^{\text{measured}}$ |
|---|---|---|
| Statistics | 0.448 | 0.448 |
| $\Delta\phi$ template and Expected number of bkg | 0.049 | 0.049 |
| $A_{gg}/A_{q\bar{q}}$ | 0.014 | 0.014 |
| Estimation method of Systematic | 0.020 | 0.020 |
| Other (top $P_t$ PYTHIA vs HERWIG) | 0.03 | 0.03 |
| | if Positive value | if Negative value |
| NLO matrix element | $0.032 \times F_{gg}^2 + 0.080 \times F_{gg} - 0.008$ | $0.032 \times F_{gg}^2 + 0.080 \times F_{gg} - 0.008$ |
| PDF | $0.068 \times F_{gg}^2 - 0.009 \times F_{gg} + 0.027$ | $-0.046 \times F_{gg}^2 + 0.009 \times F_{gg} - 0.040$ |
| | $\pm$ half of the largest | |
| ISRFSR more | $-0.054 \times F_{gg}^2 - 0.067 \times F_{gg} + 0.049$ | $-0.054 \times F_{gg}^2 - 0.067 \times F_{gg} + 0.049$ |
| ISRFSR less | $-0.004 \times F_{gg}^2 - 0.061 \times F_{gg} + 0.098$ | $-0.004 \times F_{gg}^2 - 0.061 \times F_{gg} + 0.098$ |

TABLE III: The summary table of systematic. When the polarity matches, NLO matrix element and ISR less systematics are made to add.

### H. Summary of Uncertainty

## VI. RESULT

Finally, we reveal $\Delta\phi$ distribution of the data sample after we fixed the analysis method and studies of systematic uncertainties.

Figure 9 indicates the distribution of $\Delta\phi$ in 2.0 fb$^{-1}$ data (left). The solid curve on the histogram means the best fit. The solid line on the confidence belt (right) indicates $\mathcal{F}_{gg}^{\text{measured}}$ and its cross section with the confidence belt corresponds to the confidence interval on $\mathcal{F}_{gg}^{\text{true}}$. From this, we retrieve the following results:

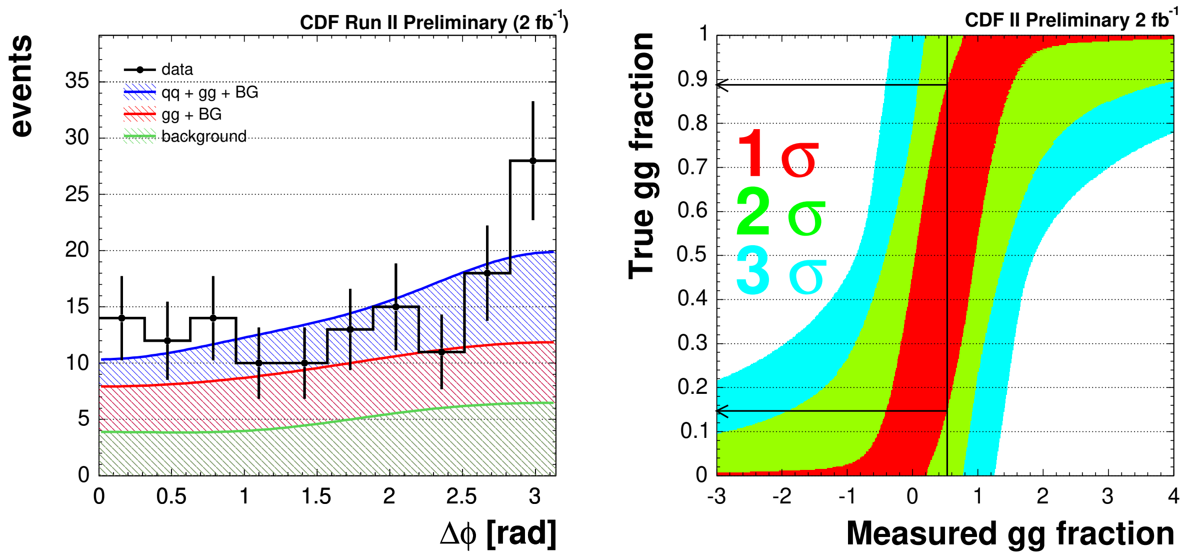


FIG. 9: The distribution of $\Delta\phi$ in 2.0 fb$^{-1}$ data (left). The solid curve on the histogram means the best fit. The solid line on the confidence belt (right) indicates $\mathcal{F}_{gg}^{\text{measured}}$ and its cross section with the confidence belt corresponds to the confidence interval on $\mathcal{F}_{gg}^{\text{true}}$.

$$\mathcal{F}_{gg} \;=\; 0.53\,^{+0.36}_{-0.38}\;\left(^{+0.35}_{-0.37}(stat.)^{+0.07}_{-0.08}(+syst.)\right) \tag{2}$$

**Acknowledgments**

We thank the Fermilab staff and the technical staffs of the participating institutions for their vital contributions. This work was supported by the U.S. Department of Energy and National Science Foundation; the Italian Istituto Nazionale di Fisica Nucleare; the Ministry of Education, Culture, Sports, Science and Technology of Japan; the Natural Sciences and Engineering Research Council of Canada; the National Science Council of the Republic of China; the Swiss National Science Foundation; the A.P. Sloan Foundation; the Bundesministerium fuer Bildung und Forschung, Germany; the Korean Science and Engineering Foundation and the Korean Research Foundation; the Particle Physics and Astronomy Research Council and the Royal Society, UK; the Russian Foundation for Basic Research; the Comision Interministerial de Ciencia y Tecnologia, Spain; and in part by the European Community's Human Potential Programme under contract HPRN-CT-20002, Probe for New Physics.

---

[1] N. Kidonakis et al., Phys, Rev. D **68** 2003 114014; M. Cacciari et al., J.High Energy Phys. **0404** 2004 068
[2] T. Arens, et al., Phys, Lett. B **302** 1993 501-506
[3] Y. Hara, Prog, Theor. Phys. **86** 1991 779
[4] D.Acosta et al., Phys, Rev, Lett. **93** 142001 (2004)
[5] W. Bernreuther et al., Nucl. Phys. B **690** 2004 81-137
[6] S. Frixione and B.R. Webber, J. High Energy Phys. **0206** 2002 029; S. Frixione et al., J. High Energy Phys. **0308** 2003 007
[7] F. Abe, et al., Nucl. Instrum. Methods Phys. Res. A **271**, 387 (1988); D. Amidei, et al., Nucl. Instum. Methods Phys. Res. A **350**, 73 (1994); F. Abe, et al., Phys. Rev. D **52**, 4784 (1995); P. Azzi, et al., Nucl. Instrum. Methods Phys. Res. A **360**, 137 (1995); The CDFII Detector Technical Design Report, Fermilab-Pub-96/390-E
[8] T. Sjostrand et al., High-Energy-Physics Event Generation with PYTHIA 6.1, Comput. Phys. Commun. **135**, 238 (2001).
[9] G. Corcella et al., HERWIG 6: An Event Generator for Hadron Emission Reactions with Interfering Gluons (including supersymmetric processes), JHEP **01**, 10 (2001).